Aerosol and Air Quality Research, 16: 885–899, 2016

ISSN: 1680-8584 print / 2071-1409 online
doi: 10.4209/aaqr.2015.06.0391

Towards a Universal "Baseline" Characterisation of Air Masses for High- and Low-Altitude Observing Stations Using Radon-222

Scott D. Chambers[1*], Alastair G. Williams[1], Franz Conen[2], Alan D. Griffiths[1], Stefan Reimann[3], Martin Steinbacher[3], Paul B. Krummel[4], L. Paul Steele[4], Marcel V. van der Schoot[4], Ian E. Galbally[4], Suzie B. Molloy[4], John E. Barnes[5]

[1] *Australian Nuclear Science & Technology Organisation, Locked Bag 2001, Kirrawee DC, NSW, 2232, Australia*
[2] *Environmental Geosciences, University of Basel, Bernoullistrasse 30, 4056 Basel, Switzerland*
[3] *Laboratory for Air Pollution & Environmental Technology (Empa), Swiss Federal Laboratories for Materials Science and Technology, Überlandstrasse 129, CH-8600, Dübendorf, Switzerland*
[4] *CSIRO Oceans and Atmosphere Flagship, Aspendale, Victoria, 3195, Australia*
[5] *NOAA/Mauna Loa Observatory, Hilo, HI, USA*

ABSTRACT

We demonstrate the ability of atmospheric radon concentrations to reliably and unambiguously identify local and remote terrestrial influences on an air mass, and thereby the potential for alteration of trace gas composition by anthropogenic and biogenic processes. Based on high accuracy (lower limit of detection 10–40 mBq m^{-3}), high temporal resolution (hourly) measurements of atmospheric radon concentration we describe, apply and evaluate a simple two-step method for identifying and characterising constituent mole fractions in baseline air. The technique involves selecting a radon-based threshold concentration to identify the "cleanest" (least terrestrially influenced) air masses, and then performing an outlier removal step based on the distribution of constituent mole fractions in the identified clean air masses. The efficacy of this baseline selection technique is tested at three contrasting WMO GAW stations: Cape Grim (a coastal low-altitude site), Mauna Loa (a remote high-altitude island site), and Jungfraujoch (a continental high-altitude site). At Cape Grim and Mauna Loa the two-step method is at least as effective as more complicated methods employed to characterise baseline conditions, some involving up to nine steps. While it is demonstrated that Jungfraujoch air masses rarely meet the baseline criteria of the more remote sites, a selection method based on a variable monthly radon threshold is shown to produce credible "near baseline" characteristics. The seasonal peak-to-peak amplitude of recent monthly baseline CO_2 mole fraction deviations from the long-term trend at Cape Grim, Mauna Loa and Jungfraujoch are estimated to be 1.1, 6.0 and 8.1 ppm, respectively.

Keywords: ^{222}Rn; Clean air; Mountain site; Terrestrial influence; Greenhouse gases.

INTRODUCTION

A first step toward accurately gauging cumulative long-term natural and anthropogenic influences on the mean state of the global or hemispheric atmosphere, or to assessing the efficacy of existing mitigation strategies (locally or globally), is reliable identification of "baseline" conditions. For the purposes of this study, baseline here refers to well-mixed air masses that have had minimal recent influence from localised processes which emit or remove trace species, and are therefore characterised by concentrations of constituent trace species that can be considered representative of tropospheric regional or hemispheric mean or background values. The methodical characterisation of trends in baseline concentrations of trace constituents is also critical for quantitative assessment of individual pollution events on sub-synoptic timescales, objective model evaluation (since typical ground based measurements can be highly variable and representative of only a fraction of a model's grid-cell volume) and providing constrained input to model inversions (e.g., Brooks *et al.*, 2012).

To this end, a global network of atmospheric baseline monitoring stations is maintained as part of the World Meteorological Organisation's (WMO) Global Atmosphere Watch (GAW) program. These stations are specifically located with the intention of providing regionally representative measurements relatively free of significant local pollution sources (WMO/GAW, 2007). To maximise

* Corresponding author.
Tel.: +61-2-9717-3058
E-mail address: szc@ansto.gov.au

compatibility of the long-term datasets and the representativeness of baseline values, at least within hemispheres, it is important that baseline selection criteria are devised in a consistent or transparent manner. However, consistent definition of baseline conditions across the network of WMO GAW sites has historically been problematic since they represent a mixture of contrasting settings: continental sites, oceanic sites, coastal sites, and high altitude sites in both continental and oceanic regions; not all of which provide the same opportunities for observing air masses that have been minimally perturbed by terrestrial contact on diurnal, synoptic or seasonal timescales. At stations where it is impractical to seek baseline conditions, a suitable compromise is typically to define "background" values, for which the presence of short-lived species, or obvious local contributions, are minimised (e.g., Calvert 1990; Parrish *et al.*, 2012).

Radon (^{222}Rn) is a naturally occurring radioactive gas with a history of use as an atmospheric tracer spanning more than a century (e.g., Wigand and Wenk, 1928, Liu *et al.*, 1984; Polian *et al.*, 1986; Jacob and Prather, 1990; Kritz *et al.*, 1990; Whittlestone *et al.*, 1998; Biraud *et al.*, 2000; Zahorowski *et al.*, 2004; Williams *et al.*, 2009, 2011; Chambers *et al.*, 2014; and references therein). It originates exclusively from the earth's surface, with a source function relatively well constrained in space and time that is typically 2–3 orders of magnitude greater from unsaturated/unfrozen land surface than from open water bodies (Wilkening and Clements, 1975; Turekian *et al.*, 1977; Schery *et al.*, 1989; Jacob *et al.*, 1997). Since it is unreactive and poorly soluble, to a good approximation the sole sink of atmospheric radon is radioactive decay. With its half-life of 3.8 days, radon can be considered a fairly conservative tracer for convective boundary layer (CBL; e.g., Williams *et al.*, 2011) and nocturnal boundary layer (NBL; e.g., Perrino *et al.*, 2001; Williams *et al.*, 2013; Chambers *et al.*, 2015a, b) mixing studies, it does not accumulate in the atmosphere on timescales of longer than a month, and typical rates of vertical atmospheric mixing result in large (order of magnitude) gradients between the atmospheric boundary layer (ABL) and the free troposphere, and also between the troposphere and stratosphere (e.g., Chambers *et al.*, 2013).

While the characteristics of radon make it an ideal and versatile tool for a variety of transport and mixing studies, the fact that it is an unambiguous indicator of recent (2–3 week) contact of an air mass with land make radon an incredibly powerful tool for atmospheric baseline studies (e.g., Griffiths *et al.*, 2014; Molloy and Galbally, 2014; Chambers *et al.*, 2015c). Since by far the majority of anthropogenic atmospheric pollution has terrestrial origins, observations of atmospheric radon provide arguably the clearest indication of the *potential* for an air mass to be polluted of any contemporary atmospheric tracer.

Historically, most studies that have employed radon as an indicator of terrestrial influence for baseline studies, have done so in conjunction with other meteorological quantities (e.g., Gras and Whittlestone, 1992; Yver *et al.*, 2011; Molloy and Galbally, 2014). The application of radon in this way has been largely as a result of limitations in instrument accuracy, together with large data exclusion rates when radon thresholds much below 100 mBq m^{-3} were employed. However, relatively recent advances in continuous atmospheric radon measurement technology (e.g., Yver *et al.*, 2011; Chambers *et al.*, 2014; Pal *et al.*, 2015; Williams and Chambers, 2015) have enabled far more stringent radon thresholds to be adopted (e.g., Chambers *et al.*, 2015c), opening up new possibilities for baseline monitoring.

Taking into account variability in the (very small) oceanic radon source function (e.g., Hoang and Servant, 1972; Peng *et al.*, 1974; Schery *et al.*, 2004) due to factors including wind speed and sea state (e.g., Nightingale *et al.*, 2000; Woolf, 2005), it has been estimated that marine boundary layer (MBL) air that has reached equilibrium with the ocean surface (3 weeks or more without land contact) is expected to have a radon concentration between 20–40 mBq m^{-3} (Zahorowski *et al.*, 2013). Consequently, air masses with radon concentrations of 50 mBq m^{-3} or more can be unambiguously identified as having experienced some degree of "recent" (less than 3 weeks) or "glancing" (brief) contact with land surfaces (i.e., potentially polluted). Conversely, air masses with radon concentrations less than 50 mBq m^{-3} have either been in long term equilibrium with the ocean surface, or have been removed from any surface-based sources for a long period (e.g., have resided for a long time in the troposphere or stratosphere before descending to the measurement site).

In this study we compare long-term, hourly atmospheric observations from three WMO GAW global stations with strongly contrasting locations: (1) Cape Grim in Tasmania, a coastal site bordering the Southern Ocean; (2) Mauna Loa Observatory, an oceanic high altitude island site in the central Pacific Ocean; and (3) Jungfraujoch, a continental high-altitude site in Europe. We investigate the behaviour of selected trace constituent mole fractions as a function of radon-defined terrestrial influence, and propose a simple, objective radon-based approach for the identification of minimally terrestrially perturbed air masses that can be universally applied regardless of site location. At sites such as Jungfraujoch, where minimum levels of terrestrial influence are at least a factor of four greater than the baseline threshold for remote sites, radon concentrations can nevertheless be used to assess the extent of recent land contact that has been experienced by the "cleanest" air masses that can be identified, in order to derive representative "background" atmosphere characteristics.

METHODS

Sites and Observations

To facilitate direct intercomparison between our findings and existing baseline investigations, this study will focus on previously published long-term datasets collected at three WMO GAW stations: Cape Grim Observatory (CGO; Tasmania, Australia), Mauna Loa Observatory (MLO; Hawaii, USA), and Jungfraujoch (JFJ; Switzerland). The CGO dataset spans the 9-year period 2004–2013 (see also Chambers *et al.*, 2015c), the MLO dataset spans the 7-year period 2004–2011 (see also Chambers *et al.*, 2013), and

the JFJ dataset spans the 2-year period 2010–2012 (see also Griffiths *et al.*, 2014).

The Cape Grim Observatory (40°41′00″S, 144°41′22″E) is situated on the remote northwest coast of Tasmania. Dominant air mass fetch types for this site include: mid- to long-term terrestrial fetch (1–4 days) over the Australian mainland, short-term terrestrial fetch (≤ 1 day) over the island of Tasmania, and long-term fetch (days to weeks) over the Southern Ocean. Conditions typically cycle between each of these fetch types on synoptic timescales (less than 2 weeks), such that a statistically significant representation of each major fetch type can be observed every month of the year. Radon sampling is conducted from ~160 m above sea level (a.s.l.; 70 m above ground level from a 90 m bluff), well within the expected variability in marine boundary layer depth for the region (400–1900 m; Zahorowski *et al.*, 2013). While this baseline station has been operational since 1976, the radon program only commenced in 1980 (see Williams and Chambers 2015 for further details). Radon is presently sampled at this site using a 5000 L detector for which the counting error at a concentration of 10 mBq m^{-3} for an hourly count is approximately 40%.

The Mauna Loa Observatory (19°32′10″N, 155°34′34″W) is situated approximately 3400 m a.s.l. on the northern flank of the Mauna Loa Volcano (4170 m a.s.l.) on the Big Island of Hawaii. Located above the typical height of the regional MBL (400–2500 m; Chambers *et al.*, 2013), it is nominally a lower tropospheric sampling site. Three kinds of air mass fetch are common at this site: (1) tropospheric air masses with distant terrestrial fetch, around 6000 km from Asia, or 4000 km from continental North America; (2) surface-influenced air masses with a direct local terrestrial fetch, as a result of convection over the Hawaiian Island chain, or anabatic/katabatic winds along the flanks of the Mauna Loa volcano; and (3) oceanic air from the MBL or tropospheric air masses without recent land contact. Unlike at CGO, not all of these fetch types are represented evenly, or to the same degree, in observations throughout the year. While local terrestrial fetch conditions can arise in any season (to varying degrees), clean oceanic air masses are uncommon in spring, and distant terrestrial fetch is uncommon in summer, peaks in early spring, and switches from being predominantly of Asian origin in winter and spring, to North American in autumn (e.g., Zahorowski *et al.*, 2005; Chambers *et al.*, 2013). While baseline monitoring at MLO began in 1956, the first radon observations were not made here until the 1990s (Hutter *et al.*, 1995; Chambers *et al.*, 2013). Radon is presently sampled at this site using a 1500 L detector for which the counting error at a concentration of 25 mBq m^{-3} for an hourly count is approximately 30%.

The high altitude research station at Jungfraujoch (46° 32′53″N, 7°59′02″E) is situated in a saddle-point on the northwest flank of the Swiss Alps at 3454 m a.s.l. The air reaching the station is often very "clean" because its elevation is well above the typical range of ABL depths over the low-lying regions either side of the Alps (Nyeki *et al.*, 2000; Ketterer *et al.*, 2014). However, the influences of complex vertical transport processes typical of mountainous terrain (e.g., Weissmann *et al.*, 2005; Rotach and Zardi, 2007) are never completely absent, and so there is always some degree of residual terrestrial influence present. A mixture of European terrestrial fetch signatures is brought to this site by a variety of vertical transport processes, including: increased boundary-layer depth due to the presence of active cumulus; anabatic winds on the flanks of the Alps; orographically induced flows (including Föhn winds); and deep convection or frontal uplift of air masses to the troposphere upstream of the station (e.g., Zellweger *et al.*, 2003; Griffiths *et al.*, 2014). The frequency and intensity of each of these processes varies seasonally, and typically results in the least terrestrial influence on JFJ air masses in winter; though not "clean" in a baseline sense. Influences of this kind on tropospheric air over complex topography make the data from Alpine sites difficult to fully utilise in inverse models, when compared with flat sites (Stohl *et al.*, 2009). Atmospheric research at JFJ commenced in 1931 (Leuenberger and Flückiger, 2008), but the radon program has only been active since December 2009. It should be noted that intermittent radon pollution from nearby train tunnels is evident in the JFJ radon record between 2012 and 2015. Radon is presently sampled at this site using a 700 L detector for which the counting error at a concentration of 40 mBq m^{-3} for an hourly count is approximately 30%.

Dual-Flow-Loop Two-Filter Radon Detectors

In contrast to proxy techniques using radon progeny measurements, dual-flow-loop two-filter radon detectors provide a direct measurement of ambient radon concentrations (Whittlestone and Zahorowski, 1998; Chambers *et al.*, 2014; Williams and Chambers, 2015). As such, the observations are subject to no assumptions regarding the degree of equilibrium between radon and its progeny (e.g., Xia *et al.*, 2010), and are not influenced significantly by precipitation, fog, aerosol loading, or changes in roughness of fetch regions.

Sampled air is first delayed by 5–6 minutes to remove the short-lived gaseous radioisotope thoron (^{220}Rn; $t_{1/2}$ = 55.6 s) from the airstream. The air is then filtered to remove ambient radon and thoron progeny, all of which are particulate, and passed into a large (e.g., 700, 1500 or 5000 L) delay volume. The sampling flow rate is set to exchange the volume of air in the delay chamber every 20 minutes, during which time new radon progeny form. An internal flow loop operates at approximately 4–5 times the sampling flow rate in order to maximise the number of newly formed radon progeny that are trapped for counting on a second filter before they decay or plate-out on the detector walls or internal components. This measurement configuration typically results in a detection level for an hourly count that is almost an order of magnitude lower than that of other common techniques of direct radon measurement (e.g., electrostatic precipitation, lower limit of detection, LLD = 160 mBq m^{-3}; Wada *et al.*, 2012).

All detectors are calibrated monthly by injecting radon for 5 hours from a Radium-226 source (±4%; PYLON Electronics), and the coefficient of variability on monthly calibrations of baseline station radon detectors is between 2–6%. Instrumental background checks are performed quarterly,

and the typical standard deviation of a 1-hour background count is equivalent to ~5 mBq m^{-3}. At an ambient radon concentration of 10 mBq m^{-3}, the counting error of the 5000 L CGO detector for an hourly count is around 40%. This uncertainty decreases as $\sim N^{-1/2}$ (for N hourly samples), and also decreases for higher radon concentrations (see also Chambers *et al.*, 2014). For the smaller volume detectors we estimate a 30% counting error at 25 mBq m^{-3} (for the 1500 L detector at MLO), and 40 mBq m^{-3} (for the 700 L detector at JFJ).

RESULTS

Seasonal Variability of Terrestrial influence at Each Station

Comparing radon observations from the three baseline stations over a whole year highlights the different absolute levels and the contrasting seasonality of terrestrial influence on their respective air masses (Fig. 1).

At CGO (Fig. 1(a)), each of the three main fetch categories (oceanic: Rn < 50 mBq m^{-3}; short-term terrestrial: 50 ≤ Rn < 1000 mBq m^{-3}; and long-term terrestrial: Rn ≥ 1000 mBq m^{-3}) are generally well represented in each month of the year. While a slight bias toward higher terrestrial influence is evident in the (austral) autumn and winter, this is not large enough to prevent the estimation of a statistically robust baseline signal in any month of the year, as evident from the consistently low monthly 10th percentile values (typically 20–30 mBq m^{-3}).

At MLO (Fig. 1(b)), it is clear that not all major fetch types are equally represented each month. For the 2010 example shown here, significant distant terrestrial influences (Rn ≥ 200 mBq m^{-3}) due to upper-level outflow events from continental Asia (e.g., Kritz *et al.*, 1990; Zahorowski *et al.*, 2005; Chambers *et al.*, 2013) are mostly restricted to the period January through April.

Throughout the remainder of the year a mix of oceanic air (Rn < 50 mBq m^{-3}) and local terrestrial influence (50 ≤ Rn < 200 mBq m^{-3}) is evident. Local radon contributions at MLO, directly related to patterns of anabatic and katabatic flow on the face of the Mauna Loa volcano, typically result in radon enhancements of ≥ 40 mBq m^{-3} above baseline (Chambers *et al.*, 2013). From February through April, monthly 10th percentile radon concentrations at MLO are of order 50–70 mBq m^{-3}, which could potentially make it difficult to define a statistically robust baseline signal for these months of the year.

At JFJ (Fig. 1(c)), the monthly 10th percentile radon concentrations in 2010 varied from 370–1100 mBq m^{-3}, and monthly minimum hourly radon concentrations never dropped below 180 mBq m^{-3}. This indicates that it is not possible at JFJ to observe air masses that have been free of significant terrestrial influence for a long period (Rn ≤ 50 mBq m^{-3}), particularly in spring and summer during fair weather conditions, when deep convection is common throughout the low-lying areas surrounding the Alps, and upslope (anabatic) mountain winds are common during the days (Henne *et al.*, 2005; Griffiths *et al.*, 2014).

Using Radon to Demonstrate Terrestrial Influence on Pollutants

Cape Grim Observatory

Since radon and most key atmospheric trace species have predominantly surface-based sources and/or sinks, the degree of terrestrial influence on an air mass as indicated by the radon concentration should be closely related to concentrations of trace species of anthropogenic (or terrestrial) origin.

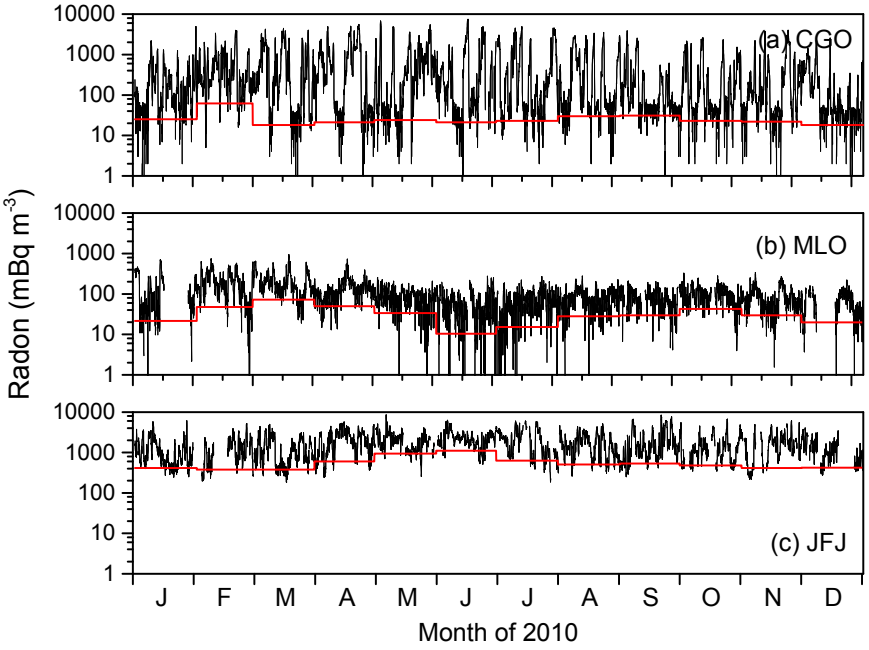

Fig. 1. Hourly radon concentrations at (a) CGO, (b) MLO, and (c) JFJ, for 2010, with monthly 10th percentile values superimposed in red. Note the logarithmic ordinate scales.

Since we were seeking to characterise the effects of recent (< 1 month) terrestrial influence on air masses, the monthly mean constituent mole fractions (based on all valid hourly observations) were removed prior to analysis to avoid seasonal variability, that is predominantly driven by other processes, biasing the results. Mean mole fractions are therefore reported as deviations from their monthly mean values. It should be noted that, since removing the monthly mean is not equally as effective at suppressing seasonality from all gases (e.g., CO_2 vs. O_3), not all deviations will appear equally distributed about zero.

Nine years (2004–2013) of the deviations of hourly observations at CGO were grouped into 5 mBq m^{-3} radon concentration bins. We then calculated average mole fractions of selected constituents (CO, CO_2, O_3 and CH_4) in each of these bins and summarised the results in Fig. 2.

For all constituents, both the highest magnitudes and the highest variability of mole fraction deviations are exhibited by air masses that experienced long-term terrestrial influence (Rn > 4000 mBq m^{-3}; Fig. 2 insets) and therefore had the longest potential exposure to terrestrially based processes. The variability in constituent mole fractions gradually decreases with decreasing terrestrial influence (radon concentrations decrease from 4000 to 1000 mBq m^{-3}) until finally, for low levels of terrestrial influence (Rn < 500 mBq m^{-3}), the variability in mean constituent mole fraction deviations becomes relatively small. Trace species mole fractions for this range of values are likely to be dominated by the larger-scale background value of the Southern Hemisphere MBL. In the case of CO_2, a plateau value is reached in this range, whilst the other species exhibit local minima (CO, CH_4) or maxima (O_3) around 20–40 mBq m^{-3} (see Figs. 2 and 3). Below about 20 mBq m^{-3}, a change in behaviour is noted in the constituent mole fractions of each of the selected species which is thought to be related to the downward transport of aged tropospheric air to the MBL in the vicinity of CGO (Chambers *et al.*, 2015c).

Fig. 3 shows distributions of the CO_2 mole fractions in the region below the "traditional" baseline radon threshold of 100 mBq m^{-3} for CGO. Instead of showing just the 9-year composite mean value for each radon bin, as in Fig. 2, in these results the binning of CO_2 mole fraction deviations from the monthly mean has been performed separately for each of the 9 years. The distributions are represented by the 10^{th}, 50^{th} and 90^{th} percentiles for each yearly bin, which are shown in green, black and red, respectively. The distribution

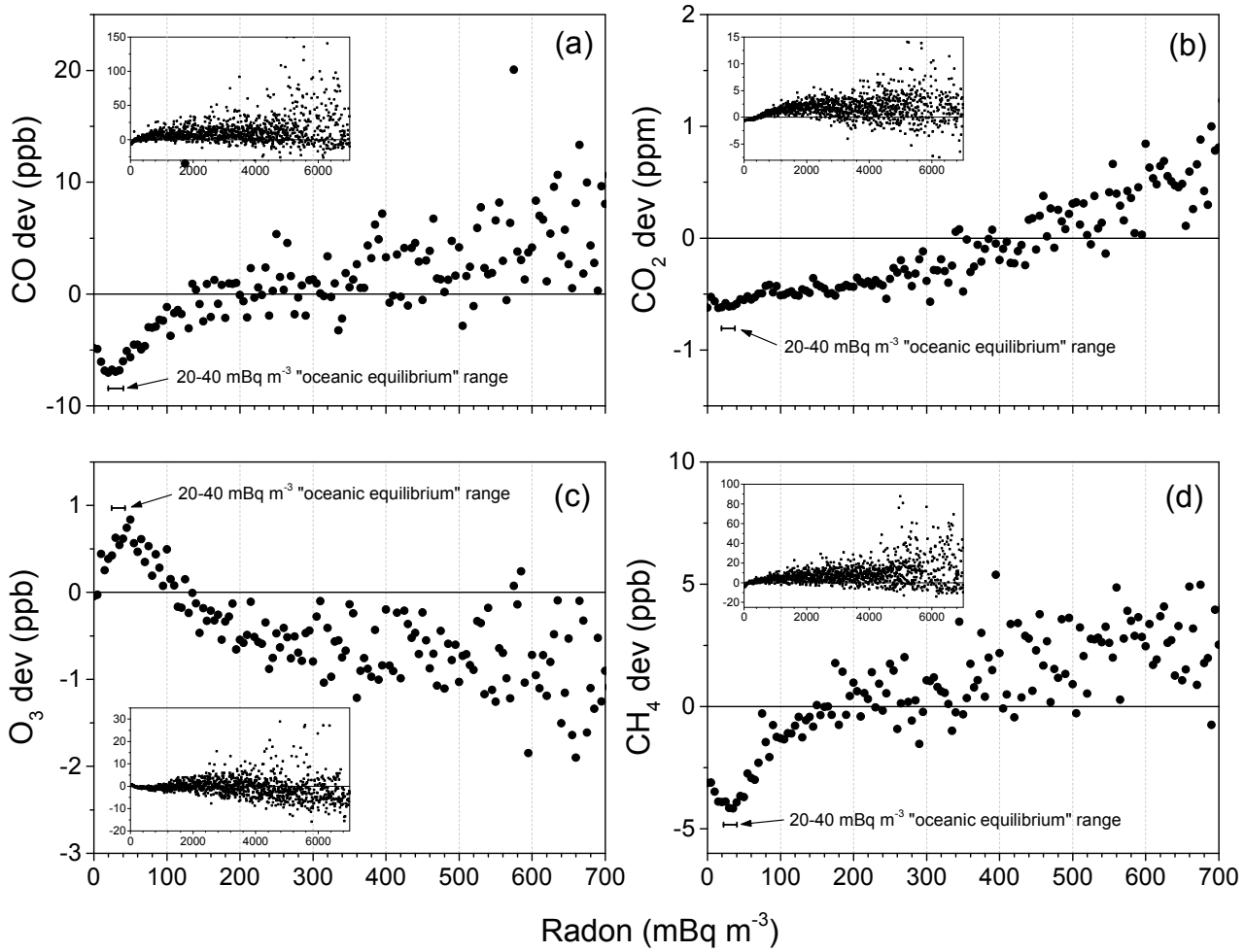

Fig. 2. Average mole fraction deviations (from monthly mean) of (a) CO, (b) CO_2, (c) O_3 and (d) CH_4 within 5 mBq m^{-3} radon concentration bins at CGO (2004–2013). Insets show results for the full range of observed radon concentrations.

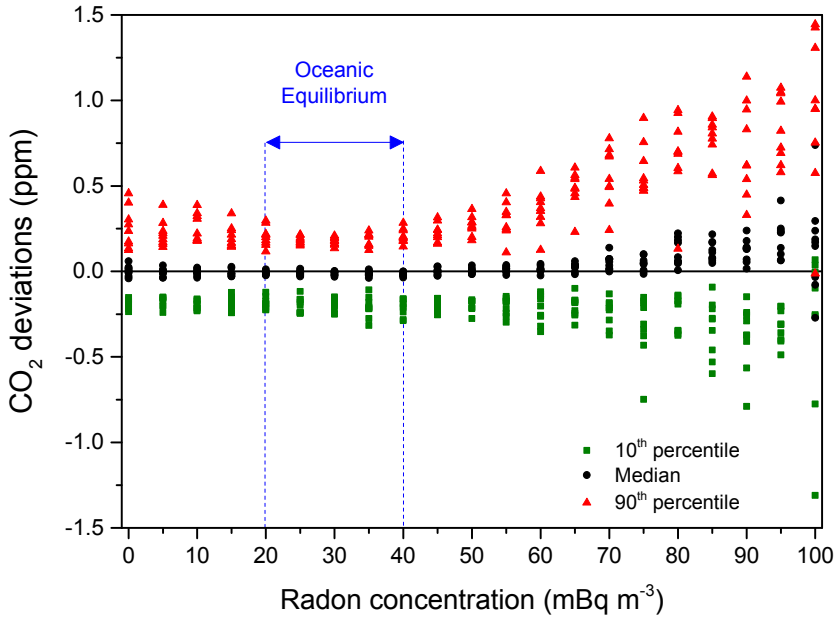

Fig. 3. CO_2 mole fraction deviations from the seasonally varying baseline value, shown as distributions (10^{th}, 50^{th}, 90^{th} percentiles) in 5 mBq m^{-3} radon bins for each year at CGO (2004–2013). Adapted from Chambers *et al.* (2015c).

of deviations about zero differs in Fig. 3 compared to Fig. 2 because, instead of simply removing monthly mean values to calculate the deviations, a varying baseline signal was constructed by linearly interpolating between monthly baseline estimates, and this curve subtracted from the hourly observations. Both Fig. 2 (bin means) and Fig. 3 (bin medians) indicate an increase in CO_2 of about 0.2 ppm from baseline conditions to air masses with radon concentrations of 100 mBq m^{-3}.

Air masses with radon concentrations in the range 20 ≤ Rn ≤ 40 mBq m^{-3} exhibited the narrowest distributions of CO_2 deviations. This range of radon concentrations is thought to be representative of mid-latitude MBL air masses that have been in long-term equilibrium with the ocean (Zahorowski *et al.*, 2013). The broadening distributions of CO_2 deviations for higher radon concentrations (Rn > 50 mBq m^{-3}) reflect the slowly increasing terrestrial influence. For Rn ≤ 20 mBq m^{-3}, on the other hand, the broadening distributions are likely attributable to tropospheric or stratospheric intrusions to the MBL in the vicinity of CGO. Chambers *et al.* (2015c) demonstrated that representative baseline mole fractions of constituent species can be retrieved from the CGO record by setting a radon concentration threshold of around 40 to 50 mBq m^{-3}, and then performing a simple outlier removal on the remaining constituent mole fractions by retaining only the 10^{th} to the 90^{th} percentile values of the selected data.

Mauna Loa Observatory

An analysis of hourly MLO observations similar to that shown in Fig. 2 was conducted for the period 2004–2011 (Fig. 4). Results were quite different for each of the three species analysed (CO_2, CH_4 and O_3). In the case of CO_2, bin-mean mole fraction deviations plateaued for radon concentrations < 150 mBq m^{-3}. However, comparatively stable bin-mean ozone mole fractions were not observed until the radon concentration had dropped to 60–70 mBq m^{-3}, and CH_4 only stabilized below radon concentrations of around 30 mBq m^{-3}. These results indicate that a similar baseline selection method to that described by Chambers *et al.* (2015c) for CGO may also be suitable for MLO observations, although based on the mole fraction variability within baseline (Figs. 3, 4(b), 4(c) and 4(f)), revised outlier removal thresholds for MLO will be required; this prospect is further investigated in the following section. Ozone mole fractions in air masses with Rn < 20 mBq m^{-3} were higher than those for air masses with 20 ≤ Rn ≤ 40 mBq m^{-3} (although by less than 5%), which may be linked to stratospheric injection.

It is of interest to note in Fig. 4 that the relative stability of bin mean values decreases significantly above radon concentrations of 200–250 mBq m^{-3}. This may represent a demarcation between local terrestrial influences, and large remote terrestrial influences.

Jungfraujoch Observatory

The results of a similar analysis on the 2-year JFJ dataset are presented in Fig. 5. Bearing in mind the complexity of the topographic setting of this site, and variety of potential vertical transport processes, we included more constituent species in the analysis to assist interpretation.

Clear reductions of constituent mole fraction deviations, and variability of their bin-mean values, are noted with decreasing terrestrial influence, as was the case for the other sites. However, in contrast to CGO and MLO, JFJ radon concentrations rarely drop below 200 mBq m^{-3}.

Water vapour mixing ratios (Fig. 5(a)) drop below their typical monthly mean values at intermediate levels of terrestrial influence (around 1500 mBq m^{-3}). Below radon concentrations of ~700 mBq m^{-3} the mixing ratio begins to

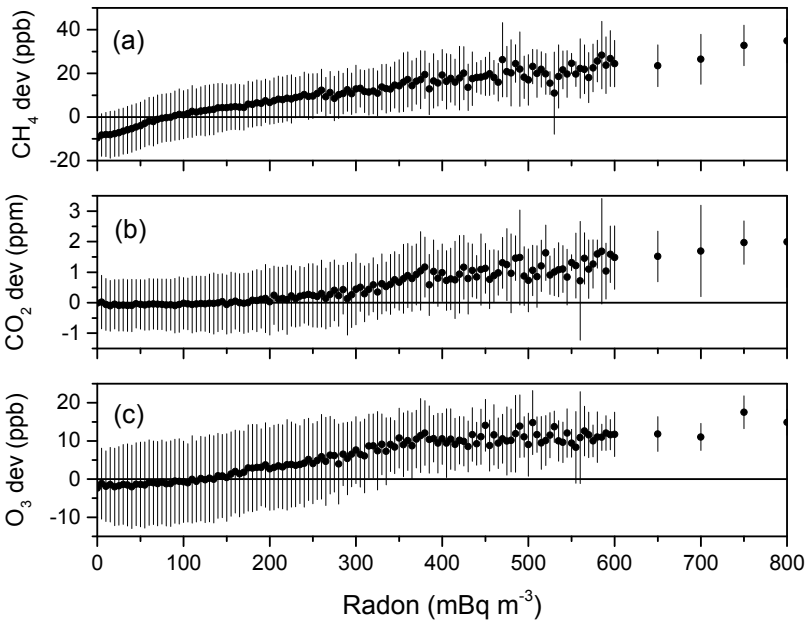

Fig. 4. Average hourly mole fraction deviations (from monthly mean values) for (a) CH_4, (b) CO_2, and (c) O_3, in 5 mBq m^{-3} radon concentration bins at MLO (2004–2011).

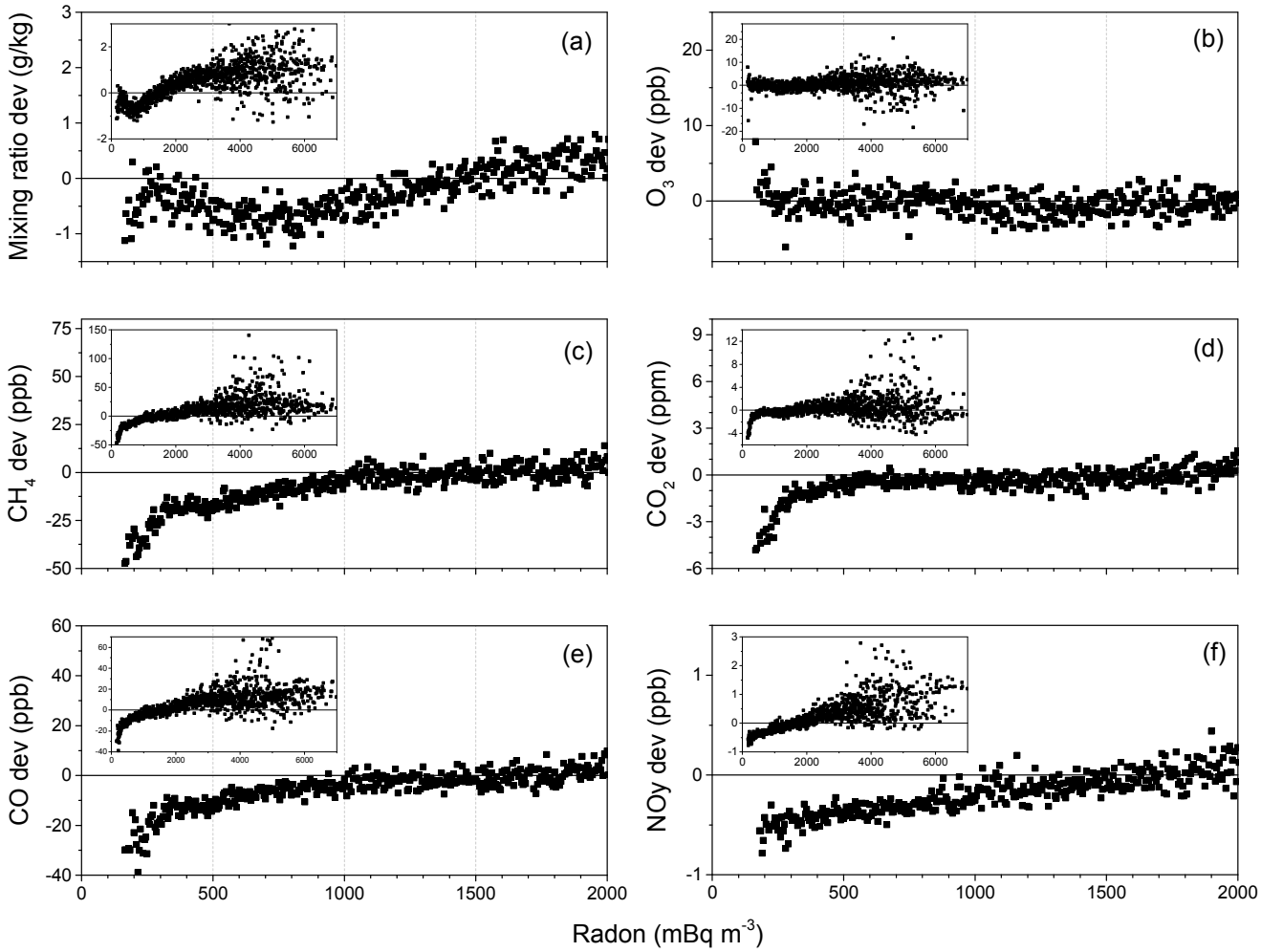

Fig. 5. Average hourly deviations from monthly mean values of: (a) water vapour mixing ratio, (b) O_3, (c) CH_4, (d) CO_2, (e) CO, and (f) reactive oxides of nitrogen (NO_y), in 5 mBq m^{-3} radon concentration bins, at JFJ (2010–2012).

increase once more, possibly indicative of air masses that have had a predominantly oceanic fetch prior to rapid transport to JFJ. Below radon concentrations of 280–300 mBq m^{-3}, the mixing ratio drops quite steeply, indicative of aged tropospheric or stratospheric air. Variability of bin-mean ozone deviations is largest for radon concentrations above 2000 mBq m^{-3}, and deviations increase at the lowest radon concentrations (≤ 250 mBq m^{-3}), as would be expected if the origin of these drier air masses was the upper troposphere or stratosphere. For the other constituent species, there is a marked change in air mass characteristics for radon concentrations between 300–1000 mBq m^{-3} (e.g., Fig. 5).

Based on the results of Fig. 5 it is likely that JFJ air masses with radon concentrations above 2000 mBq m^{-3} primarily represent boundary-layer air from the surrounding low-lying areas that has been recently transported to JFJ (e.g., through deep convection, anabatic flow, forced flow over the terrain, or frontal passages). Conversely, air masses with radon concentrations from 300–1000 mBq m^{-3} are likely representative of terrestrial boundary-layer air that was lifted to the troposphere some distance upstream of JFJ, and then advected to the site in the troposphere. Air masses with radon concentrations between 1000–2000 mBq m^{-3} are likely to be a mixture of these contributions. For radon concentrations below 300 mBq m^{-3}, the least terrestrially influenced air masses observable at JFJ, mole fractions of all tracers (except O_3) decrease sharply with respect to their monthly mean values. From this it can be deduced that, of all the JFJ observations, air masses with radon concentrations < 300 mBq m^{-3} will most closely represent baseline constituent mole fractions. Baseline radon concentrations estimated for Atlantic Ocean MBL air masses (~40 mBq m^{-3}; Biraud *et al.*, 2000), are consistent with Southern Ocean MBL air masses that have reached long-term equilibrium with the ocean surface (Zahorowski *et al.*, 2013). However, since none of the species mole fraction deviations in Fig. 5 showed signs of a plateau or minimum value (as for the other sites at low radon concentrations), any approximation of "clean" or background air characteristics at JFJ will not be a baseline value in the traditional sense (i.e., no significant identifiable terrestrial influence). Implications for the approximation of a baseline signal using JFJ observations is investigated further in the next section.

Baseline Characterisation at MLO and JFJ

Selection Process

At CGO, monthly 10th percentile radon concentrations are consistently below the proposed new baseline threshold radon concentration of around 40 to 50 mBq m^{-3}, so representative baseline estimates are possible for every month of the year. A radon-based technique for baseline characterisation at CGO, and its efficacy, has already been discussed by Chambers *et al.* (2015c). In summary, this technique employed a radon concentration threshold of 40 mBq m^{-3} as the primary baseline selection criteria, and then removed outlier values by excluding the top and bottom 10% of the distribution of trace species mole fractions for all air masses with $0 \leq Rn \leq 40$ mBq m^{-3}.

As indicated by Fig. 4, a similar radon threshold to that employed at CGO should be applicable for MLO baseline observations. Based on a 7-year composite (Fig. 6(a)), monthly 10th percentile MLO radon concentrations are below 40 mBq m^{-3} (the expected oceanic equilibrium value) for 10 months of the year. Consequently, statistically robust baseline estimates should be possible throughout most of the year, although this may not always be the case during March and April when remote terrestrial influences are most common and pronounced due to mid-troposphere continental Asian "outflow" events (e.g., Zahorowski *et al.*, 2005; Chambers *et al.*, 2013). As a baseline definition for MLO, we therefore selected all observations each month where radon concentrations were ≤ 40 mBq m^{-3}. Within this collection of least-terrestrially-perturbed air masses the distribution of constituent mole fractions will still reflect varying degrees of terrestrial influence (e.g., in the case of CO_2, biospheric uptake, or anthropogenic emissions). For the purpose of this study we employed an extreme form of the 10th/90th percentile outlier removal described by Chambers *et al.* (2015c) and selected *only* the median trace constituent mole fraction each month of all air masses with radon concentrations ≤ 40 mBq m^{-3} as a representative estimate of baseline values.

At JFJ, on the other hand, Fig. 5 suggests that the best representation of baseline constituent mole fractions would be derived from air masses with radon concentrations below 300 mBq m^{-3}. However, as can be seen in Fig. 6(b), the 10th percentile radon concentrations at JFJ are well above this threshold for much of the year. In fact, it is unlikely that statistically robust estimates of baseline constituent mole fractions could be achieved at JFJ from April through November if a constant threshold of 300 mBq m^{-3} were used. Zellweger *et al.* (2003) and Cui *et al.* (2011) report a similar seasonal shift from predominantly remote influences in winter, to predominantly local boundary-layer influences in summer at JFJ. Consequently, unlike for CGO and MLO, it may not be possible to define a baseline for minimal terrestrial influence at JFJ using a constant (seasonally independent) radon threshold. We therefore suggest a more "forgiving" definition for the baseline at JFJ, by selecting the least terrestrially influenced air masses observed each month, based on lowest monthly 10th percentile radon values. A campaign- or species-specific outlier removal procedure could then be used to exclude those air parcels that have been most significantly affected by relatively recent emissions. For the purpose of this study, we apply the same extreme form of outlier removal used for MLO of selecting only the median constituent mole fraction from the distribution of air masses with radon concentrations below the 10th percentile value. If a mole fraction range for a given trace species was required for near baseline air masses selected in this way, the "median only" constraint employed here could be relaxed as far as the 2nd to 3rd quartiles (i.e., retaining only the 25th to the 75th percentile constituent mole fractions for air masses with radon below the monthly 10th percentile value).

Constituent Mole Fractions

The results of the MLO baseline selection process are provided in Fig. 7 for the case of CO_2. The amplitude of

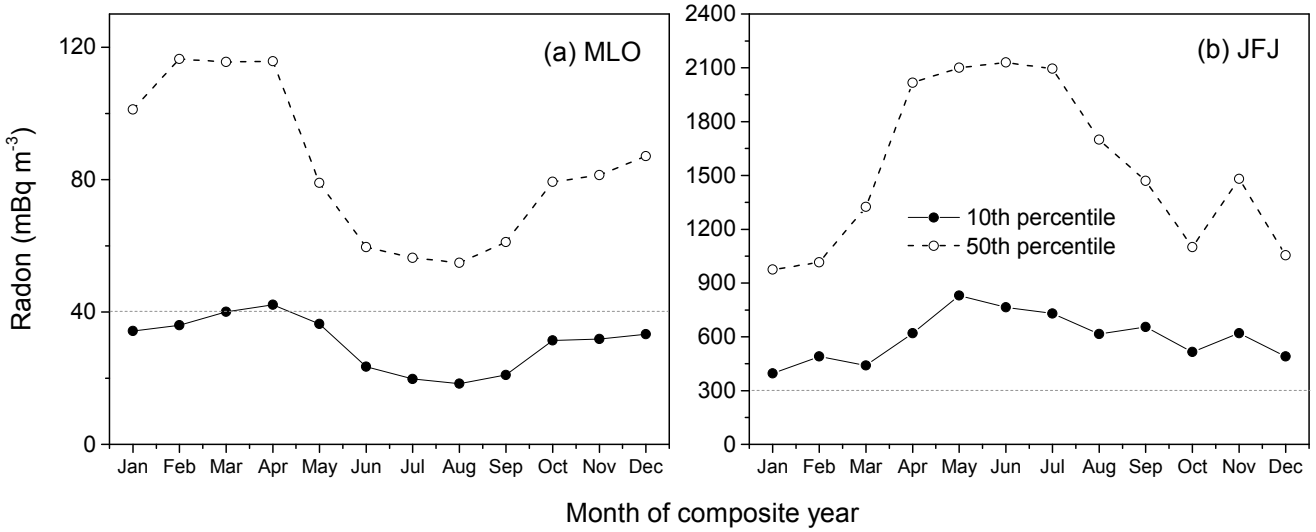

Fig. 6. Monthly median and 10th percentile radon concentrations for (a) Mauna Loa, and (b) Jungfraujoch, based on a composite year from all available data.

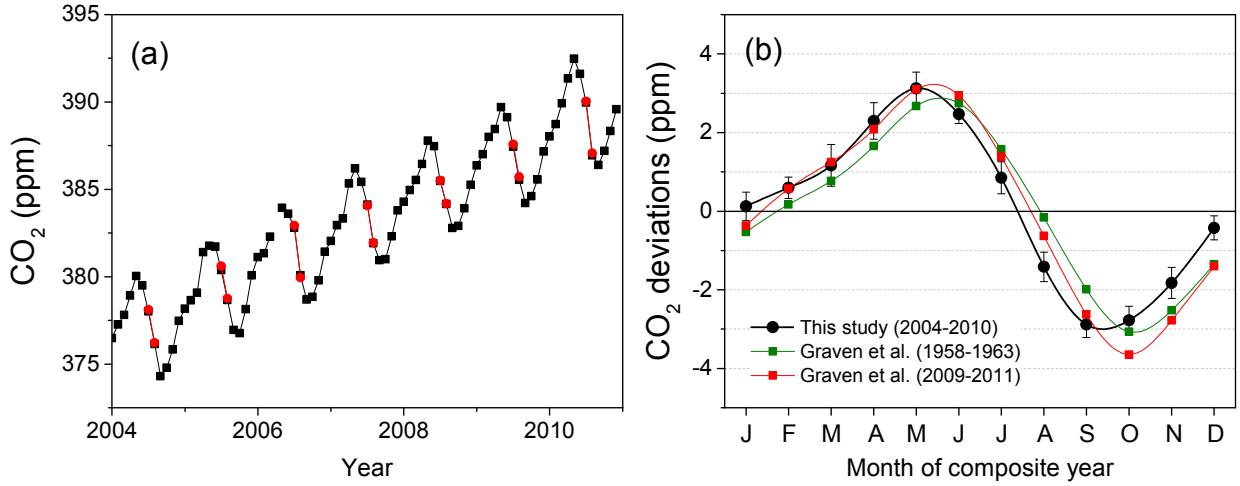

Fig. 7. Baseline CO_2 mole fractions from MLO for 2004–2010: (a) monthly values (July and August marked in red), and (b) composite year based on deviations from a 7-year linear trend (whiskers indicate ± 1σ). CO_2 cycles of Graven *et al.* (2013) also plotted for comparison.

the detrended composite baseline CO_2 signal over the 7-year period (2004-2010), presented in Fig. 7(b), falls between the MLO CO_2 seasonal cycles for the periods 1958–1963 and 2009–2011 presented by Graven *et al.* (2013), for which the data selection methods are outlined in Tans and Thoning (2008) and Keeling *et al.* (1996). It should be noted, however, that for our "pilot study" here of the radon-based technique, only a simple linear trend was removed from the 7-year MLO CO_2 record, resulting in a distribution about the mean in Fig. 7(b) that is shifted by about +0.6 ppm relative to the plots of Graven *et al.* (2013). For more detailed analyses a harmonic fit (e.g., Thoning *et al.*, 1989) would be more appropriate for removing the long-term trend. A comprehensive overview of statistical baseline techniques for observations at mountainous sites is also provided by Brooks *et al.* (2012).

We know from Fig. 6(a) (also extensively discussed in Zahorowski *et al.*, 2005; Chambers *et al.*, 2013) that the least terrestrial influence on air masses at MLO occurs in July and August. Assuming that these periods yield the most uniform aged tropospheric air masses, constituent mole fractions for air masses with Rn ≤ 40 mBq m^{-3} during these months (shown in red, Fig. 7(a)) should be the most well suited to represent long-term trends in baseline values representative of the northern hemisphere. According to Fung (2013), however – and also indicated by the detrended composite plot of Fig. 7(b) – these months are in the middle of the northern hemisphere biospheric uptake period, a period of rapid change in the northern hemisphere background CO_2.

At JFJ, we made two estimates (BL01 and BL02) of baseline constituent mole fractions using the radon observations: BL01 represents the monthly median constituent mole fractions for air masses with radon concentrations below 300 mBq m^{-3} (based on the results of

Fig. 5); and BL02 represents the median constituent mole fractions for air masses with radon concentrations below the monthly 10th percentile value. Baseline estimates for the cases of CO and CH_4 are presented in Fig. 8.

Almost without exception, the baseline estimate derived from the lowest 10th percentile of terrestrial influence on JFJ air masses (BL02) yielded constituent mole fractions substantially below the monthly mean values. However, for most months when radon concentrations below 300 mBq m^{-3} were observed, the BL01 baseline constituent estimates demonstrate that the BL02 values are still far from what might be observed in Atlantic baseline air (i.e., Rn ~40 mBq m^{-3}; Biraud *et al.*, 2000).

The smallest differences between the BL01 and BL02 estimates for CO and CH_4 (Fig. 8) occurred between December and April; cooler months when convective uplift to the lower troposphere, and anabatic winds, are less prevalent (e.g., Griffiths *et al.*, 2014). Consequently, judicious selection of constituent mole fraction information from air masses with radon concentrations below the monthly 10th percentile value for these 5 months of the year may be well suited to characterise long-term (multi-year) trends in baseline constituent mole fractions.

Based on the change in air mass characteristics evident for Rn < 1000 mBq m^{-3} (e.g., Figs. 5(c) and 5(e)), an alternative use of the JFJ observations may be to define a "continental background" signal for comparison with global Chemical Transport Model estimates of lower tropospheric constituent mole fractions over central Europe. Here, background air masses are understood to contain minimal short-lived species, or evidence of local influences (e.g., Calvert, 1990; Parrish *et al.*, 2012). Griffiths *et al.* (2014) demonstrated that a radon threshold of 1000 mBq m^{-3} at JFJ was very effective for producing representative background aerosol scattering coefficients.

Comparing Baseline Signals between Stations

Radon derived baseline CO_2 mole fractions at MLO and the two JFJ baseline approximations are compared for 2010 in Fig. 9. A 45% larger amplitude and 30° phase shift is apparent in the JFJ baseline approximations compared with MLO. This may be attributable to the larger terrestrial influence on selected air masses at JFJ, or it may be due to a latitudinal variation, Graven *et al.* (2013) demonstrated a 157% increase in amplitude (7 to 18 ppm) and a 45° phase shift (of the annual CO_2 minimum) of the Northern Hemisphere baseline CO_2 signal with latitude increasing from Mauna Loa to Barrow.

The amplitude of the radon-derived Southern Hemisphere baseline CO_2 signal from CGO is approximately a factor of 5 less than that observed at MLO and 180° out of phase (Fig. 10(a)). However, the minimum mole fractions track very closely over the 7-year observation period, indicating matching long-term growth rates. Biospheric uptake in the northern hemisphere is sufficiently strong to reduce baseline CO_2 mole fractions at MLO below the corresponding CGO values in the northern hemisphere summer. Baseline CH_4 mole fractions at CGO are on average ~50 ppb lower than at MLO (Fig. 10(b)). While the seasonal cycles are of a more comparable amplitude, it is much more regular at CGO, reflecting a reduced diversity of sources and sinks in the Southern Hemisphere, and the dominant effect of the seasonal removal of CH_4 by reaction with the hydroxyl radical in the Northern Hemisphere.

Comparison of Radon-Derived Baseline Estimates with Previous Studies

As noted in Section 3.3.2, CO_2 baseline deviation estimates reported by Graven *et al.* (2013) for the period 2009–2011 were not significantly different from those of this study over the period 2004–2010 (Fig. 8(b)). A completely independent MLO baseline selection method to that employed in the present study was outlined by Chambers *et al.* (2013). This technique selected air masses that had not made landfall beyond the Pacific Basin in the previous 10 days, that had not interacted with the marine boundary layer in transit,

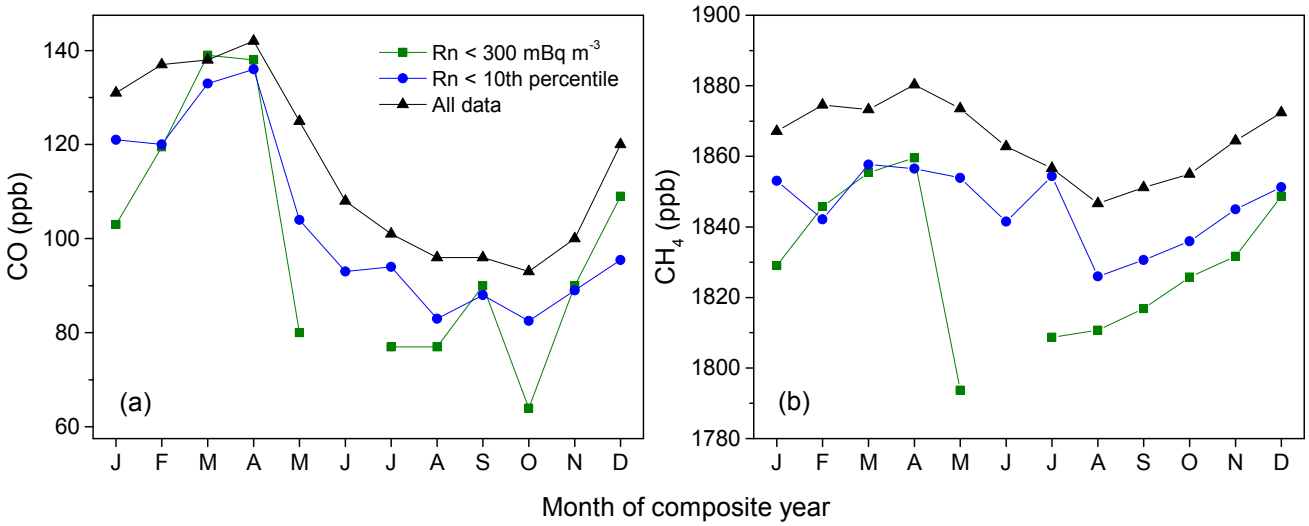

Fig. 8. Composite monthly mean mole fractions of (a) CO, and (b) CH_4 at JFJ (black triangles). Monthly baseline estimates (BL01, blue circles; BL02, green squares) are also shown.

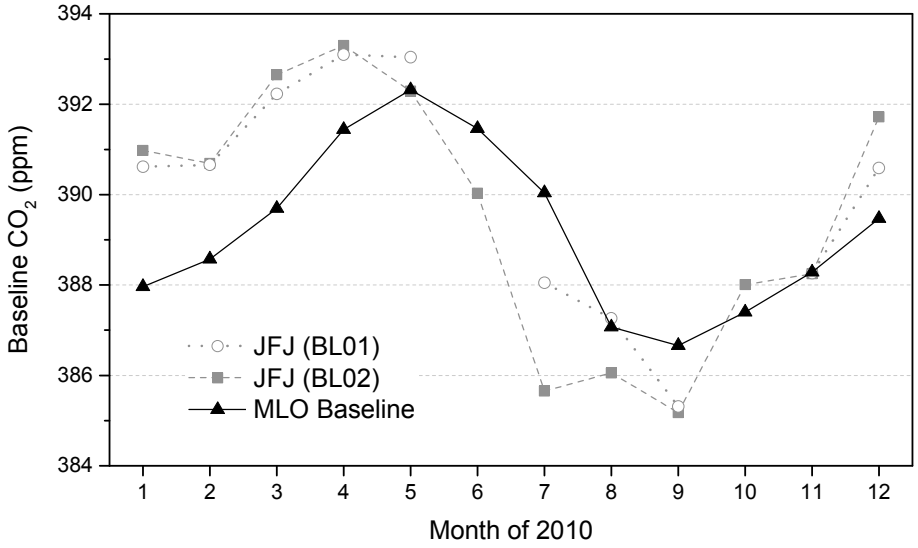

Fig. 9. Comparison of radon-derived baseline CO_2 mole fraction between MLO and JFJ for 2010.

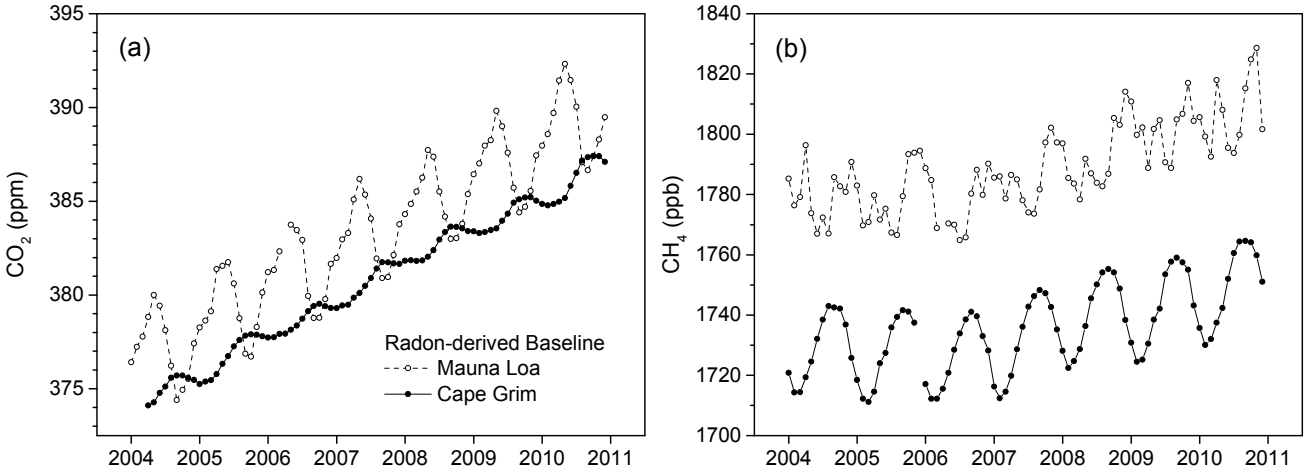

Fig. 10. Comparison of radon-derived baseline (a) CO_2 and (b) CH_4 mole fraction estimates between MLO and CGO from 2004 to 2011.

had not dropped below station height (3.4 km) in the vicinity of the Hawaiian Island chain, were slow moving, and arrived at MLO within a restricted (0800–1000 h LST) temporal window (to minimize effects associated with local topographically-driven circulations). Monthly MLO baseline CO_2 estimates from the present study and Chambers *et al.* (2013) are compared in Fig. 11. Despite the comparative simplicity of the two-step baseline selection process employed in the present study (constant radon threshold and median CO_2 value; ignoring even the traditionally assumed need for a diurnal sampling window on mountain sites) the findings are remarkably similar.

While the MLO baseline selection technique of Chambers *et al.* (2013) likely yields a more representative baseline value, the difference is small, and the two-step process described here is easier to apply. Furthermore, even a slight relaxation of the median-only outlier removal process described here would exclude a much smaller data fraction than the approach of Chambers *et al.* (2013), which yielded only 9 hourly valid baseline samples per month (on average over the 7-year period.

At JFJ, a variety of selection baseline criteria have previously been employed, including a $[NO_y]/[CO]$ ratio of 0.008 (Pandey Deolal *et al.*, 2013), a time-of-day filter ($0200 \leq UTC \leq 0800h$; Andrews *et al.*, 2011), a fixed 500 mBq m^{-3} radon threshold (Xia *et al.*, 2013), statistical approaches (Ruckstuhl *et al.*, 2012), meteorological/synoptic filters (e.g., Forrer *et al.*, 2000; Collaud *et al.*, 2011), and filters based on air mass origin derived from trajectory analysis (Balzani-Lööv *et al.*, 2008; Cui *et al.*, 2011). As demonstrated in Griffiths *et al.* (2014), the constant radon threshold of 500 mBq m^{-3} (750 mBq m^{-3} STP) was more successful than the time-of-day filter and produced results consistent with the $[NO_y]/[CO]$ method for estimating monthly values for the baseline aerosol scattering coefficient. Based on the results of Fig. 5, however, air masses with radon concentrations of 500 mBq m^{-3} can still contain non-negligible terrestrial/anthropogenic influence; although this

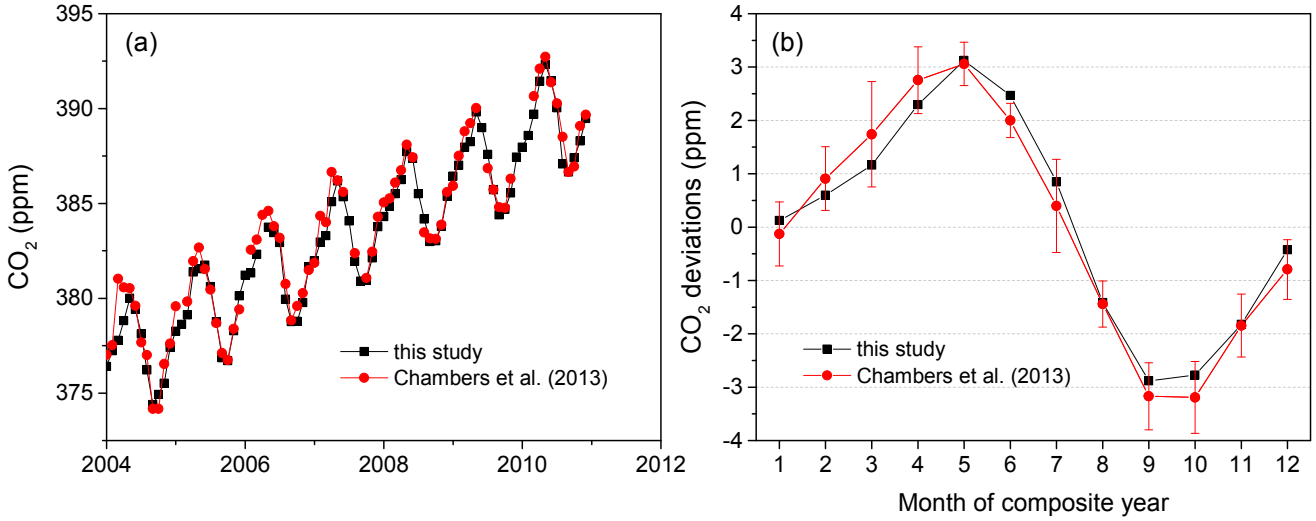

Fig. 11. Comparison of radon-derived baseline CO_2 mole fractions estimates at MLO between this study and Chambers *et al*. (2013). Whiskers represent ± 1σ of monthly baseline estimates, and the standard deviation of results from this study shown in Fig. 7(b).

influence is likely to be from more distant sources. For the period December through March, the BL01 method (see Fig. 6(b), solid black squares) is comparable to the 500 mBq m^{-3} threshold of Xia *et al.* (2013), but Fig. 8 shows that when a sufficient number of lower radon concentrations are available, the BL02 method (300 mBq m^{-3}) would yield constituent mole fractions closer to a "true baseline" value. However, adopting the 300 mBq m^{-3} threshold constitutes a huge reduction in monthly data yield and may not be well suited to all studies.

CONCLUSIONS

Radon-222 (radon), a versatile natural atmospheric tracer, is demonstrated to reliably identify local and remote terrestrial influences on an air mass. Since the majority of anthropogenic trace species sources are of terrestrial origin, high-quality atmospheric radon observations therefore provide a valuable guide as to the potential an air mass has for its composition to be altered.

A simple two-step approach for identifying and characterising constituent mole fractions in baseline air is described and tested at three WMO GAW stations in very different locations and settings (Cape Grim, Tasmania; Mauna Loa, Hawaii; and Jungfraujoch, Switzerland). To enable comparison of findings between stations, and facilitate intercomparison with existing baseline estimates, partially-overlapping previously published datasets were used: Cape Grim Observatory (Jan-2004 to Dec-2012); Mauna Loa Observatory (Jan-2004 to Dec-2010); and Jungfraujoch (Jan-2010 to Dec-2011).

The technique involves selecting a radon-based threshold concentration to identify the "cleanest" (least terrestrially influenced) air masses, and then performing an outlier removal step based on the distribution of constituent mole fractions in the identified clean air masses. At the coastal (CGO) and remote-island (MLO) sites, air masses with minimal terrestrial influence (Rn ≤ 40 mBq m^{-3} "true baseline") were well represented each month of the year. At the continental JFJ site, however, air masses were rarely observed with Rn < 200 mBq m^{-3}, limiting even observations of the cleanest possible air to "near baseline". Consequently, seasonally independent radon thresholds could be applied year-round at CGO and MLO year-round, whereas a variable (monthly) threshold had to be adopted at JFJ.

Exceptional agreement was achieved between these results and previously published baseline estimates, despite the large variety of baseline selection techniques that have historically been used. In particular, the diurnal windowing technique that is commonly used at mountain sites was not employed in the current study. These results demonstrate that, when observations of sufficient accuracy and temporal resolution are available, radon by itself can provide a simple and powerful alternative to existing baseline selection techniques. Importantly, as demonstrated at JFJ, radon can be used as an effective indicator of relative terrestrial influence (or pollution potential) for estimating constituent concentrations in "background" air at sites not ideally situated for baseline observations. In subsequent studies the performance of this technique will be evaluated in more detail and for a wider range of site characteristics.

ACKNOWLEDGEMENTS

The authors would like to thank Ot Sisoutham and Sylvester Werczynski at the Australian Nuclear Science and Technology Organisation for their support of the radon measurement programs at all stations, and the technical and support staff at the Cape Grim Observatory in Tasmania. We are also indebted to the staff at the Mauna Loa Observatory, particularly Paul Fukumura, for their ongoing assistance, and acknowledge the ongoing help and support of the National Oceanic and Atmospheric Administration, Earth System Research Laboratory, Global Monitoring

Division, specifically Ed Dlugokencky, Pieter Tans, Kirk Thoning, and Samuel Oltmans, for access to hourly CH_4, CO_2, and O_3 records. Last, but not least, we would like to thank the International Foundation High Alpine Research Stations Jungfraujoch and Gornergrat (HFSJG) for making it possible for us to carry out our measurements at the High Alpine Research Station Jungfraujoch. Measurements at Jungfraujoch are financially supported by the Swiss Federal Office for the Environment and ICOS (Integrated Carbon Observation System)-Switzerland.

REFERENCES

Andrews, E., Ogren, J., Bonasoni, P., Marinoni, A., Cuevas, E., Rodríguez, S., Sun, J., Jaffe, D., Fischer, E., Baltensperger, U., Weingartner, E., Coen, M.C., Sharma, S., Macdonald, A., Leaitch, W., Lin, N.H., Laj, P., Arsov, T., Kalapov, I., Jefferson, A. and Sheridan, P. (2011). Climatology of Aerosol Radiative Properties in the Free Troposphere. *Atmos. Res.* 102: 365–393.

Balzani-Lööv, J.M., Henne, S., Legreid, G., Staehelin, J., Reimann, S., Prévôt, A.S.H., Steinbacher, M. and Vollmer, M.K. (2008). Estimation of Background Concentrations of Trace Gases at the Swiss Alpine Site Jungfraujoch (3580 m asl). *J. Geophys. Res.* 113: D22305, doi: 10.1029/2007jd009751.

Biraud, S., Ciais, P., Ramonet, M., Simmonds, P., Kazan, V., Monfray, P., O'Doherty, S., Spain, T.G. and Jennings, S.G. (2000). European Greenhouse Gas Emissions Estimated from Continuous Atmospheric Measurements and Radon 222 at Mace Head, Ireland. *J. Geophys. Res.* 105: 1351–1366.

Brooks, B.G.J., Desai, A.R., Stephens, B.B., Bowling, D.R., Burns, S.P., Watt, A.S., Heck, S.L. and Sweeney, C. (2012). Assessing Filtering of Mountaintop CO_2 Mole Fractions for Application to Inverse Models of Biosphere-atmosphere Carbon Exchange. *Atmos. Chem. Phys*. 12: 2099–2115.

Calvert, J.G. (1990). Glossary of Atmospheric Chemistry Terms. *Pure Appl. Chem.* 62: 2167–2219.

Chambers, S.D., Zahorowski, W., Williams, A.G., Crawford, J. and Griffiths, A.D. (2013). Identifying Tropospheric Baseline Air Masses at Mauna Loa Observatory between 2004 and 2010 Using Radon-222 and Back Trajectories. *J. Geophys. Res.* 118: 992–1004, doi: 10.1029/2012JD018212.

Chambers, S.D., Hong, S.B., Williams, A.G., Crawford, J., Griffiths, A.D. and Park, S.J. (2014). Characterising Terrestrial Influences on Antarctic Air Masses Using Radon- 222 Measurements at King George Island. *Atmos. Chem. Phys.* 14: 9903–9916.

Chambers, S.D., Wang, F., Williams, A.G., Xiaodong, D., Zhang, H., Lonati, G., Crawford, J., Griffiths, A.D., Ianniello, A. and Allegrini, I. (2015a). Quantifying the Influences of Atmospheric Stability on Air Pollution in Lanzhou, China, Using a Radon-Based Stability Monitor. *Atmos. Environ.* 107: 233–243.

Chambers, S.D., Williams, A.G., Crawford, J. and Griffiths, A.D. (2015b). On the Use of Radon for Quantifying the Effects of Atmospheric Stability on Urban Emissions. *Atmos. Chem. Phys.* 15: 1175–1190.

Chambers, S.D., Williams, A.G., Crawford, J., Griffiths, A.D., Krummel, P.B., Steele, L.P., Law, R.M., van der Schoot, M.V., Galbally, I.E. and Molloy, S.B. (2015c). A Radon-only Technique for Characterising "Baseline" Constituent Concentrations at Cape Grim. In *Baseline Atmospheric Program Australia 2011-2013*, Derek, N., Krummel, P.B. and Cleland, S.J. (Eds.), Australian Bureau of Meteorology and CSIRO Marine and Atmospheric Research, *in Press*. https://www.researchgate.net/publication/280028388_A_RADON-ONLY_TECHNIQUE_FOR_CHARACTERISING_ATMOSPHERIC_%27BASELINE%27_CONSTITUENT_CONCENTRATIONS_AT_CAPE_GRIM.

Collaud Coen, M., Weingartner, E., Furger, M., Nyeki, S., Prévôt, A.S.H., Steinbacher, M. and Baltensperger, U. (2011). Aerosol Climatology and Planetary Boundary Influence at the Jungfraujoch Analyzed by Synoptic Weather Types. *Atmos. Chem. Phys.* 11: 5931–5944.

Cui, J., Pandey Deolal, S., Sprenger, M., Henne, S., Staehelin, J., Steinbacher, M. and Nédélec, P. (2011). Free Tropospheric Ozone Changes over Europe as Observed at Jungfraujoch (1990–2008): An Analysis Based on Backward Trajectories. *J. Geophys. Res.* 116: D10304, doi: 10.1029/2010JD015154.

Forrer, J., Rüttimann, R., Schneiter, D., Fischer, A., Buchmann, B. and Hofer, P. (2000). Variability of Trace Gases at the High-Alpine Site Jungfraujoch Caused by Meteorological Transport Processes. *J. Geophys. Res.* 105: 12241–12251.

Fung, I. (2013). A Hyperventilating Biosphere. *Science* 341: 1075.

Gras, J.L. and Whittlestone, S. (1992). Radon and CN: Complementary Tracers of Polluted Air Masses at Coastal and Island Sites. *J. Radioanal. Nucl. Chem.* 161: 293–306.

Graven, H.D., Keeling, R.F., Piper, S.C., Patra, P.K., Stephens, B.B., Wofsy, S.C., Welp, L.R., Sweeney, C., Tans, P.P., Kelley, J.J., Daube, B.C., Kort, E.A., Santoni, G.W. and Bent, J.D. (2013). Enhanced Seasonal Exchange of CO_2 by Northern Ecosystems Since 1960. *Science* 341: 1085.

Griffiths, A.D., Conen, F., Weingartner, E., Zimmermann, L., Chambers, S.D., Williams, A.G. and Steinbacher, M. (2014). Surface-to-mountaintop Transport Characterised by Radon Observations at the Jungfraujoch. *Atmos. Chem. Phys.* 14: 12763–12779.

Henne S., Furger, M. and Prévôt, A.S.H. (2005). Climatology of Mountain Venting Induced Moisture Layers in the Lee of the Alps. *J. Appl. Meteorol.* 44: 620–633.

Hoang, C.T. and Servant, J. (1972). Radon Flux from the Sea (in French). *C. R. Acad. Sci. Paris* 274: 3157–3160.

Hutter, A.R., Larsen, R.J., Maring, H. and Merril, J.T. (1995). ^{222}Rn at Bermuda and Mauna Loa: Local and Distant Sources. *J. Radioanal. Nucl. Chem.* 193: 309–318.

Jacob, D.J., Prather, M.J., Rasch, P.J., Shia, R.L., Balkanski, Y.J., Beagley, S.R., Bergmann, D.J., Blackshear, W.T., Brown, M., Chiba, M., Chipperfield, M.P., de Grandpré,

J., Dignon, J.E., Feichter, J., Genthon, C., Grose, W.L., Kasibhatla, P.S., Köhler, I., Kritz, M.A., Law, K., Penner, J.E., Ramonet, M., Reeves, C.E., Rotman, D.A., Stockwell, D.Z., Van Velthoven, P.F.J., Verver, G., Wild, O., Yang, H. and Zimmermann, P. (1997). Evaluation and Intercomparison of Global Atmospheric Transport Models Using ^{222}Rn and Other Short Lived Tracers. *J. Geophys. Res.* 102: 5953–5970.

Keeling, C.D., Chin, J.F.S. and Whorf, T.P. (1996). Increased Activity of Northern Vegetation Inferred from Atmospheric CO_2 Measurements. *Nature* 382: 146–149.

Ketterer, C., Zieger, P., Bukowiecki, N., Collaud Coen, M., Maier, O., Ruffieux, D. and Weingartner, E. (2014). Investigation of the Planetary Boundary Layer in the Swiss Alps Using Remote Sensing and in Situ Measurements. *Boundary Layer Meteorol.* 151: 317–334.

Kritz, M.A. (1990). The China Clipper—Fast Advective Transport of Radon Rich Air from the Asian Boundary Layer to the Upper Troposphere near California. *Tellus Ser. B* 42: 46–61.

Leuenberger, M. and Flückiger, E. (2008). Research at Jungfraujoch. *Sci. Total Environ.* 391: 169–176.

Liu, S.C., McAfee, J.R. and Cicerone, R.J. (1984). Radon-222 and Tropospheric Vertical Transport. *J. Geophys. Res.* 89: 7291–7297.

Molloy, S.B. and Galbally, I.E. (2014). Analysis and Identification of a Suitable Baseline Definition of Tropospheric Ozone at Cape Grim, Tasmania. In *Baseline Atmospheric Program Australia 2009-2010*, Derek, N., Krummel, P.B. and Cleland, S.J. (Eds.), Australian Bureau of Meteorology and CSIRO Marine and Atmospheric Research, pp. 7–16, June 2014.

Nightingale, P.D., Malin, G., Law, C.S., Watson, A.J., Liss, P.S., Liddicoat, M.I., Boutin, J. and Upstill-Goddard, R.C. (2000). In Situ Evaluation of Air-Sea Gas Exchange Parameterizations Using Novel Conservative and Volatile Tracers. *Global Biogeochem. Cycles* 14: 373–387.

Nyeki, S., Kalberer, M., Colbeck, I., Wekker, S.D., Furger, M., Gäggeler, H.W., Kossmann, M., Lugauer, M., Steyn, D., Weingartner, E., Wirth, M. and Baltensperger, U. (2000). Convective Boundary Layer Evolution to 4 km a.s.l. over High-Alpine Terrain: Airborne Lidar Observations in the Alps. *Geophys. Res. Lett.* 27: 689–692.

Pal, S., Lopez, M., Schmidt, M., Ramonet, M., Gibert, F., Xueref-Remy, I. and Ciais, P. (2015). Investigation of the Atmospheric Boundary Layer Depth Variability and Its Impact on The ^{222}Rn Concentration at a Rural Site in France. *J. Geophys. Res.* 120: 623–643, doi: 10.1002/2014JD022322.

Pandey Deolal, S., Staehelin, J., Brunner, D., Cui, J., Steinbacher, M., Zellweger, C., Henne, S. and Vollmer, M.K. (2013). Transport of PAN and NO_y from Different Source Regions to the Swiss High Alpine Site Jungfraujoch. *Atmos. Environ.* 64: 103–115.

Parrish, D.D., Law, K.S., Staehelin, J., Derwent, R., Cooper, O.R., Tanimoto, H., Volz-Thomas, A., Gilge, S., Scheel, H.E., Steinbacher, M. and Chan, E. (2012). Long-Term Changes in Lower Tropospheric Baseline Ozone Concentrations at Northern Mid-Latitudes. *Atmos. Chem. Phys.* 12, 11485–11504.

Peng, T.H., Takahashi, T. and Broecker, W.S. (1974). Surface Radon Measurements in the North Pacific Ocean Station Papa. *J. Geophys. Res.* 79: 1772–1780.

Perrino, C., Pietrodangelo, A. and Febo, A. (2001). An Atmospheric Stability Index Based on Radon Progeny Measurements for the Evaluation of Primary Urban Pollution. *Atmos. Environ.* 35: 5235–5244.

Polian, G., Lambert, G., Ardouin, B. and Jegou, A. (1986). Long-range Transport of Continental Radon in Subantarctic and Arctic Areas. *Tellus* 38: 178–189.

Rotach, M.W. and Zardi, D. (2007). On the Boundary-layer Structure over Highly Complex Terrain: Key Findings from MAP. *Q. J. R. Meteorolog. Soc.* 133: 937–948.

Ruckstuhl, A.F., Henne, S., Reimann, S., Steinbacher, M., Buchmann, B. and Hueglin, C. (2012). Robust Extraction of Baseline Signal of Atmospheric Trace Species Using Local Regression. *Atmos. Meas. Tech. Discuss.* 5: 2613–2624.

Schery, S.D., Whittlestone, S., Hart, K.P. and Hill, S.E. (1989). The Flux of Radon and Thoron from Australian Soils. *J. Geophys. Res.* 94: 8567–8576.

Stohl, A., Seibert, P., Arduini, J., Eckhardt, S., Fraser, P., Greally, B.R., Lunder, C., Maione, M., Mühle, J., O'Doherty, S., Prinn, R.G., Reimann, S., Saito, T., Schmidbauer, N., Simmonds, P.G., Vollmer, M.K., Weiss, R.F. and Yokouchi, Y. (2009). An Analytical Inversion Method for Determining Regional and Global Emissions of Greenhouse Gases: Sensitivity Studies and Application to Halocarbons. *Atmos. Chem. Phys.* 9: 1597–1620.

Tans, P. and Thoning, K. (2008). How We Measure Background CO_2 Levels on Mauna Loa. http://www.esrl.noaa.gov/gmd/ccgg/about/co2_measurements.html. Global Greenhouse Gas Reference Network Report, Boulder, Colorado, September 2008.

Thoning, K.W., Tans, P.P. and Komhyr, W.D. (1989). Atmospheric Carbon-Dioxide at Mauna Loa Observatory. 2. Analysis of the NOAA GMCC Data, 1974-1985. *J. Geophys. Res.* 94: 8549–8565.

Turekian, K.K., Nozaki, Y. and Benninger, L.K. (1977). Geochemistry of Atmospheric Radon and Radon Products. *Annu. Rev. Earth Planet. Sci.* 5: 227–255.

Wada, A., Matsueda, H., Murayama, S., Taguchi, S., Kamada, A., Nosaka, M., Tsuboi, K. and Sawa, Y. (2012). Evaluation of Anthropogenic Emissions of Carbon Monoxide in East Asia Derived from Observations of Atmospheric Radon-222 over the Western North Pacific. *Atmos. Chem. Phys.* 12: 12119–12132.

Weissmann, M., Braun, F.J., Gantner, L., Mayr, G.J., Rahm, S. and Reitebuch, O. (2005). The Alpine Mountain–plain Circulation: Airborne Doppler Lidar Measurements and Numerical Simulations. *Mon. Weather Rev.* 133: 3095–3109.

Whittlestone, S. and Zahorowski, W. (1998). Baseline Radon Detectors for Shipboard Use: Development and Deployment in the First Aerosol Characterisation Experiment (ACE 1). *J. Geophys. Res.* 103: 16743–16751.

Whittlestone, S., Gras, J.L. and Siems, S.T. (1998). Surface Air Mass Origins during the First Aerosol Characterization Experiment (ACE 1). *J. Geophys. Res.* 103: 16341–16350.

Wigand, A., and Wenk, F. (1928). Der Gehalt der Luft an Radium-Emanation, nach Messungen bei Flugzeugaufstiegen. *Ann. Lpz. Phys.* 86: 657–686.

Wilkening, M.H. and Clements, W.E. (1975). Radon 222 from the Ocean Surface. *J. Geophys. Res.* 80: 3828–3830.

Williams, A.G. and Chambers, S.D. (2015). A History of Radon Measurements at Cape Grim. In *Baseline Atmospheric Program Australia 2011-2013*, Derek, N., Krummel, P.B. and Cleland, S.J. (Eds.), Australian Bureau of Meteorology and CSIRO Marine and Atmospheric Research, *in Press*.

Williams, A.G., Chambers, S.D. and Griffiths, A. (2013). Bulk Mixing and Decoupling of the Nocturnal Stable Boundary Layer Characterized Using a Ubiquitous Natural Tracer. *Boundary Layer Meteorol.* 149: 381–402, doi: 10.1007/s10546-013-9849-3.

Williams, A.G., Chambers, S.D., Zahorowski, W., Crawford, J., Matsumoto, K. and Uematsu, M. (2009). Estimating the Asian Radon Flux Density and Its Latitudinal Gradient in Winter Using Ground-based Radon Observations at Sado Island. *Tellus Ser. B* 61: 732–746.

Williams, A.G., Zahorowski, W., Chambers, S., Griffiths, A., Hacker, J.M., Element, A. and Werczynski, S. (2011). The Vertical Distribution of Radon in Clear and Cloudy Daytime Terrestrial Boundary Layers. *J. Atmos. Sci.* 68: 155–174.

WMO/GAW (2007). WMO/GAW Strategic Plan: 2008-2015 – A Contribution to the Implementation of the WMO Strategic Plan: 2008-2011 (WMO TD No 1384), GAW Report #172, 108 pp, July 2007, http://www.wmo.int/pages/prog/arep/gaw/gaw-reports.html).

Woolf, D.K. (2005). Parameterization of Gas Transfer Velocities and Sea-state-dependent Wave Breaking. *Tellus Ser. B* 57: 87–94.

Xia, Y., Conen, F., and Alewell, C. (2013). Total Bacterial Number Concentration in Free Tropospheric Air above the Alps. *Aerobiologia* 29: 153–159.

Xia, Y., Sartorius, H., Schlosser, C., Stöhlker, U., Conen, F. and Zahorowski, W. (2010). Comparison of One- and Two-filter Detectors for Atmospheric ^{222}Rn Measurements under Various Meteorological Conditions. *Atmos. Meas. Tech.* 3: 723–731.

Yver, C., Schmidt, M., Bousquet, P. and Ramonet, M. (2011). Measurements of Molecular Hydrogen and Carbon Monoxide on the Trainou Tall Tower. *Tellus Ser. B* 52–63.

Zahorowski, W., Griffiths, A.D., Chambers, S.D., Williams, A.G., Law, R.M., Crawford, J. and Werczynski, S. (2013). Constraining Annual and Seasonal Radon-222 Flux Density from the Southern Ocean Using Radon-222 Concentrations in the Boundary Layer at Cape Grim. *Tellus Ser. B* 65: 19622, doi: 10.3402/tellusb.v65i0.19622.

Zahorowski, W., Chambers, S., Wang, T., Kang, C.H., Uno, I., Poon, S., Oh, S.N., Werczynski, S., Kim, J. and Henderson-Sellers, A. (2005). Radon-222 in Boundary Layer and Free Tropospheric Continental Outflow Events at Three ACE-Asia Sites. *Tellus Ser. B* 57: 124–140.

Zahorowski, W., Chambers, S.D. and Henderson-Sellers, A. (2004). Ground Based Radon-222 observations and Their Application to Atmospheric Studies. *J. Environ. Radioact*. 76: 3–33.

Zellweger, C., Forrer, J., Hofer, P., Nyeki, S., Schwarzenbach, B., Weingartner, E., Ammann, M. and Baltensperger, U. (2003). Partitioning of Reactive Nitrogen (NO_y) and Dependence on Meteorological Conditions in the Lower Free Troposphere. *Atmos. Chem. Phys.* 3: 779–796.

Received for review, June 4, 2015
Revised, July 22, 2015
Accepted, July 30, 2015